Charge-density wave stacking order in 1 T-$Ta_{1-x}Zr_xSe_2$: Interlayer interactions and impurity (Zr) effects

D. E. Moncton
Bell Laboratories, Murray Hill, New Jersey 07974
and Brookhaven National Laboratory, Upton, New York 11973*

F. J. DiSalvo
Bell Laboratories, Murray Hill, New Jersey 07974

J. D. Axe
Brookhaven National Laboratory, Upton, New York 11973*

L. J. Sham
Department of Physics, University of California San Diego, La Jolla, California 92037

Bruce R. Patton†
Department of Physics, Massachusetts Institute of Technology, Cambridge, Massachusetts 02139
(Received 3 May 1976)

Ordering of the commensurate charge-density waves (CDWs) from layer to layer in 1 T-$Ta_{1-x}Zr_xSe_2$ is observed by neutron diffraction to give superlattice Bragg peaks at $2c^*/13$, $5c^*/13$, and $6c^*/13$ for $x \leq 0.015$. With larger Zr concentration ($x = 0.03$), a broad peak (full width at half maximum of $0.1c^*$) centered at $c^*/3$ is found. Nearest- and next-nearest-layer interactions are required to explain the implied stacking sequences in the pure limit. As impurities are added, the random potential dominates the next-nearest-layer interaction and a disordered CDW stacking structure develops. A simple model of this disorder is presented which accurately fits the observed scattering profiles.

I. INTRODUCTION

Charge-density waves (CDWs) are now known to develop in materials having quasi-one-dimensional[1,2] (1D) or two-dimensional[3] (2D) electronic character. As a result of weak interactions among the 1D or 2D units (i.e., chains or layers), the ground states of these systems either have, or tend to have, three-dimensional (3D) long-range order. This order can be viewed as a particular choice of CDW phase shift from unit to unit. It is thought that structural imperfection may drastically upset such ordering by randomly pinning the CDW phase to vacancies or impurities. For example, Sham and Patton[4] have recently suggested that the intrinsic disorder of the Br atoms in potassium cyanoplatinide (KCP) prevents the development of long-range order between the chains, and McMillan[5] has studied the effects of impurities using a Landau theory of the CDW transition. In addition, Sham and Patton[6] have shown generally that within the Landau theory, a random impurity field destroys long-range CDW ordering in less than four dimensions.

In this paper we report a neutron-diffraction study of the ordering among CDWs in successive layers in 1 T-$Ta_{1-x}Zr_xSe_2$ with varying impurity (i.e., Zr) concentration. In the clean limit ($x \approx 0$) the CDW superlattice has 3D long-range order. At higher Zr concentrations ($0.03 < x < 0.06$), ordering is well-described by a disordered stacking model. To successfully explain the observed structures we will consider the competition between the CDW-impurity interaction and the interlayer interactions.

In order to establish the role of impurities in the present system, it is necessary to understand the pure material. Transmission-electron-diffraction studies[3] have revealed an incommensurate CDW superlattice in 1 T-$TaSe_2$ at high temperatures, which becomes commensurate in a discontinuous transition at $T_d = 473$ K. In both phases, there are three distortion plane waves having wave vectors $\vec{q}_1$, $\vec{q}_2$, and $\vec{q}_3$ related by trigonal symmetry. The basal plane projection of the superlattice in the commensurate phase is shown in Fig. 1. The lattice parameter $a' = \sqrt{13}\,a$ is appropriate for the "unit cell" of this superlattice, which is the primary concern of the present paper. Throughout our discussion we will refer the data to the conventional hexagonal reciprocal lattice. Vectors $\vec{a}_1^*$ and $\vec{a}_2^*$ are defined in Fig. 1, and $\vec{c}^*$ is perpendicular to the layer with length $2\pi/c$.

Although 1 T-$TaSe_2$ has significant 2D anisotropy, the superlattice has 3D long-range order. Previous x-ray powder data[3,7] indicated the complexity of this superstructure. A unit cell derived to fit the data was incorrect.[7] The proper interpretation

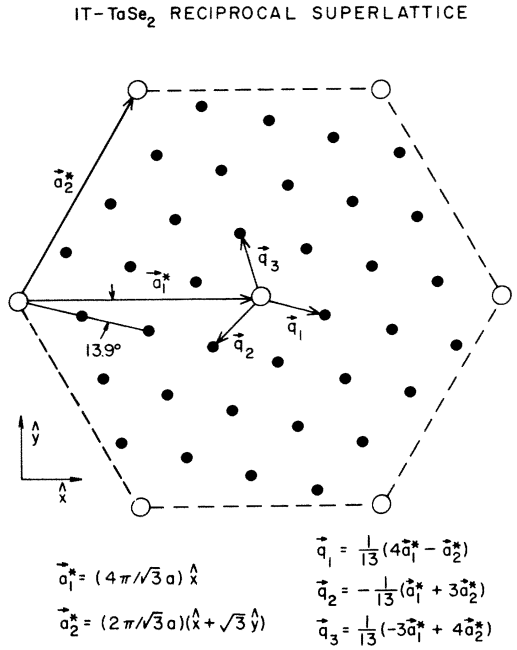

FIG. 1. Basal plane projection of the hexagonal reciprocal lattice (open circles) and the $\sqrt{13}a$ superlattice (filled circles). The three wave vectors $\vec{q}_1$, $\vec{q}_2$, and $\vec{q}_3$ comprising the CDW are shown.

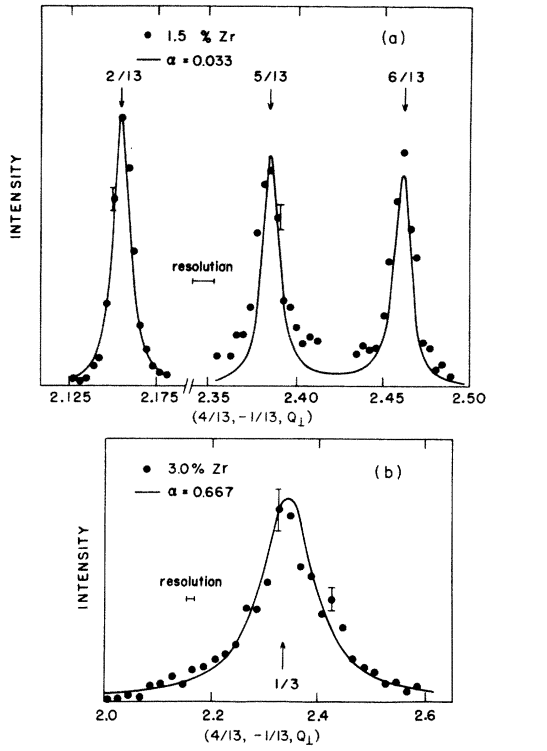

FIG. 2. Scans along $(\frac{4}{13}, -\frac{1}{13}, Q_\perp)$ in samples with Zr concentrations $x = 0.015$ (a) and $x = 0.03$ (b). Line shapes calculated using the model described in text are shown normalized to best fit the data. The two different data sets in (a) are normalized independently.

was made, however, after a suggestion by Scruby *et al.*[8] in a single-crystal x-ray study of $1T$-TaS_2 was confirmed in the present neutron experiments. Scruby *et al.* viewed the 3D superstructure as a stacking sequence in which the atomic positions in a layer are generated by translating the positions in the preceding layer by a vector $\vec{T}_i = n_i\vec{a}_1 + m_i\vec{a}_2$, where n_i and m_i are integers. Since the undistorted lattice ($1T$ structure) is invariant under this translation, the operation may be considered a translation (or phase shift) of the CDW and its concomitant lattice distortion.

II. NEUTRON-DIFFRACTION RESULTS

Elastic-neutron-diffraction ($E_0 = 14$ meV) measurements were performed on a triple-axis spectrometer (set for zero energy transfer) at the Brookhaven high-flux beam reactor. Pyrolytic graphite crystals were used for monochromator, analyzer, and filter. All data presented here were taken at 300 K. Preparation and physical properties of single-crystal samples of $1T$-$Ta_{1-x}Zr_xSe_2$ are described in a paper[9] on the effect of doping on CDWs in layered compounds. The samples used varied in size from 10 to 100 mg.

Figure 2 shows scans as a function of $\vec{Q}_\perp$ (perpendicular to layer) with $\vec{Q}_\parallel = \vec{q}_1 = \frac{4}{13}\vec{a}_1^* - \frac{1}{13}\vec{a}_2^*$. In a sample with low ($x = 0.015$) Zr concentration [Fig. 2(a)], we find narrow peaks at $\vec{Q}_\perp = (2+\frac{2}{13})\vec{c}^*$, $(2+\frac{5}{13})\vec{c}^*$, and $(2+\frac{6}{13})\vec{c}^*$. To understand the interlayer-stacking order implied by these data, we must first consider the superlattice unit cell for a single layer shown in Fig. 3. The description of the ordering requires the definition of 13 translation vectors $\vec{T}_i$ which shift the origin of the CDW to the various Ta atom sites in the figure. The sites have been numbered in a sequence given by successive translations by the vector $\vec{T}_2 = 2\vec{a}_1 + \vec{a}_2$. This vector is defined as $\vec{T}_2$ because it connects Ta site 2 to the origin (Ta site 1), but it is easily seen that, in general, it connects Ta sublattice $i+1$ to sublattice i. In Fig. 4(b) we depict a stacking sequence in which each successive layer is shifted by $\vec{T}_2$ with respect to the previous layer. Sequences may also be described by giving the translation vector for each layer relative to the first layer. In the particular sequence of Fig. 4(b), the second layer is shifted by $\vec{T}_2$, the third by $\vec{T}_3$, the fourth by $\vec{T}_4$, etc. Since each translation vector is defined only within the first supercell, one must draw extended patterns in real space to see the equivalence of the two descriptions.

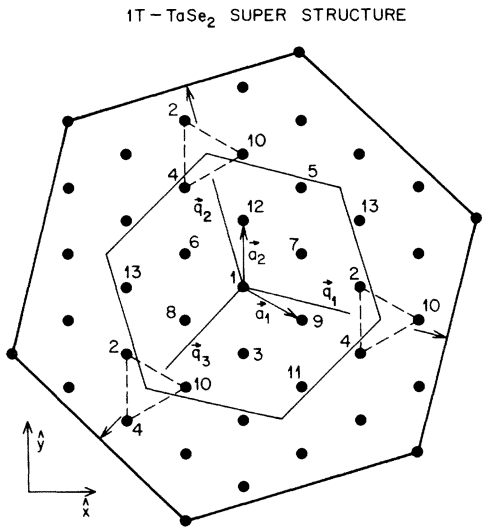

FIG. 3. Schematic representation of the CDW superstructure is superimposed on the hexagonal lattice of Ta atoms. Se atoms (not shown) are located at positions $\pm(\frac{2}{3}\vec{a}_1, \frac{1}{3}\vec{a}_2, \frac{1}{4}\vec{c})$. The inner hexagon is the primitive cell of the superstructure. The outer hexagon (heavy line) and the triangles (dashed line) connecting Ta sites 2, 4, and 10 help to interpret Fig. 4. The translation vectors $\vec{T}_i$ defined in the text connect the ith Ta site with Ta site 1 at the origin.

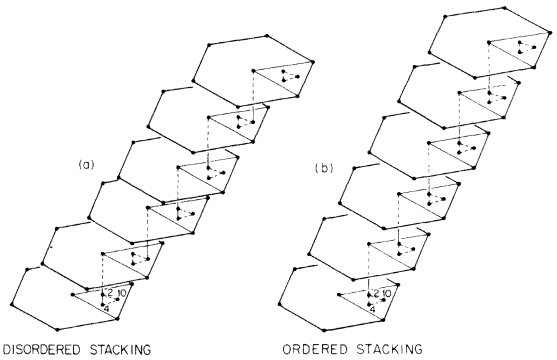

FIG. 4. Stacking models describing two extremes of CDW interlayer ordering are shown. In structure (b) CDWs have long-range order characterized by the relative translation vector $\vec{T}_2$. In case (a) a disordered CDW structure having translations $\vec{T}_2, \vec{T}_4, \vec{T}_{10}$ chosen randomly is shown.

To make connection with the data of Fig. 2(a), it is convenient to characterize the stacking superstructure of Fig. 4(b) by modifying the three wave vectors of the single-layer CDW to include a component in the $\hat{z}$ direction. We define new wave vectors of the 3D lattice as follows:

$$\vec{q}_1' = \vec{q}_1 - (\vec{q}_1 \cdot \vec{T}_2/c)\,\hat{z} = \vec{q}_1 - \tfrac{7}{13}\vec{c}^*,$$
$$\vec{q}_2' = \vec{q}_2 - (\vec{q}_2 \cdot \vec{T}_2/c)\,\hat{z} = \vec{q}_2 + \tfrac{5}{13}\vec{c}^*,$$
$$\vec{q}_3' = \vec{q}_3 - (\vec{q}_3 \cdot \vec{T}_2/c)\,\hat{z} = \vec{q}_3 + \tfrac{2}{13}\vec{c}^*.$$

Superlattice peaks occur at momentum transfers $\vec{Q} = \vec{\tau} + \vec{q}_i'$ where $\vec{\tau}$ is any reciprocal-lattice vector of the $1T$ structure. Stacking sequences derived from the vectors $\vec{T}_4$ and $\vec{T}_{10}$ are equivalent to that shown for $\vec{T}_2$ in Fig. 4(b) by trigonal symmetry. A macroscopic crystal would naturally have domains of the three stacking types. As a result, three superlattice peaks occur at fractional c^* values given by

$$-\vec{q}_1 \cdot \vec{T}_2/c = -\tfrac{7}{13}, \quad -\vec{q}_1 \cdot \vec{T}_4/c = +\tfrac{5}{13},$$
$$-\vec{q}_1 \cdot \vec{T}_{10}/c = +\tfrac{2}{13},$$

in agreement with the data of Fig. 2(a).

A question arises as to why two adjacent layers are always related by vectors $\vec{T}_2, \vec{T}_4, \vec{T}_{10}$ since there are thirteen possible translations. It is easily seen that translations from the set $(\vec{T}_2, \vec{T}_4, \vec{T}_{10})$ or the set $(\vec{T}_3, \vec{T}_5, \vec{T}_{11})$ move charge maxima in one layer farthest from similar maxima in a neighboring layer.[10] However, the trigonal symmetry of the lattice implies that different interaction energies will characterize each set. On the basis of the data we conclude that the second set $(\vec{T}_3, \vec{T}_5, \vec{T}_{11})$ must not be energetically as favorable as the set $(\vec{T}_2, \vec{T}_4, \vec{T}_{10})$.

Further analysis of the data in Fig. 2(a) shows that the peak widths are slightly greater than the instrumental resolution, which is $\Delta Q_\perp = 0.016c^*$ for all data shown. Therefore, the correlation length $\xi_\perp$ (perpendicular to the layer) must not be much longer than 150 Å, or about 25 layers ($c = 6.27$ Å). Since pure $1T$-$TaSe_2$ has long-range order,[11] we conclude that the addition of impurities has decreased the length of the stacking domains. As expected, the correlation length is further reduced in samples with larger Zr concentration. Materials with $x = 0.03$, 0.05, and 0.07 have been studied and each exhibits scattering similar to that shown for the $x = 0.03$ sample in Fig. 2(b). There is a broad Lorentzian-shaped peak centered about $\vec{Q}_\perp = (2 + \frac{1}{3})\vec{c}^*$, with a correlation length $\xi_\perp = 13.3$ Å (about two layers) for each of these concentrations.

Although the addition of Zr impurities induces a rapid decrease in $\xi_\perp$, the in-layer correlation length $\xi_\parallel$ remains long, producing peaks with widths (along $\vec{Q}_\parallel$) just larger than instrumental resolution. Crude estimates of these correlations are: $\xi_\parallel \sim 140$ Å for the $x = 0.015$ sample and $\xi_\parallel = 110$ Å for the $x = 0.05$ sample. Apparently these widths are much less sensitive to impurity concentrations in this range than those indicative of interlayer disorder.

III. CALCULATION OF SCATTERING PROFILES

As demonstrated in Fig. 2, both sets of data are well fitted by theoretical scattering profiles. These functions are derived for a model-layered system in which each layer is assumed to have a CDW with long-range coherence in the layer. The system is comprised of stacking sequences which are characterized by one translation vector from the set $(\vec{T}_2, \vec{T}_4, \vec{T}_{10})$. The sequences are separated by "stacking faults" which occur when the translation vector changes from one vector in the set to another. The probability α that a stacking fault will occur is a variable in the model. The results of calculations to be described presently are shown in Fig. 5 for four values of α. For $\alpha = 0.033$ the average number of layers between faults is $1/\alpha = 30$, and the profile fits the data of the $x = 0.015$ sample [Fig. 2(a)] where the peak width indicated a correlation length of about 25 layers. Since the instrumental resolution is not negligible, we expect that the fit would be improved by including it in the calculated profiles.

The value $\alpha = 0.667$ (or $\alpha = \frac{2}{3}$) represents complete disorder. The choice of stacking translation $\vec{T}_2$, $\vec{T}_4$, or $\vec{T}_{10}$ is made randomly in going from one layer to the next, as shown schematically in Fig. 4(a). The scattering profile calculated for this model fits the data for the sample with $x = 0.03$ [Fig. 2(b)].

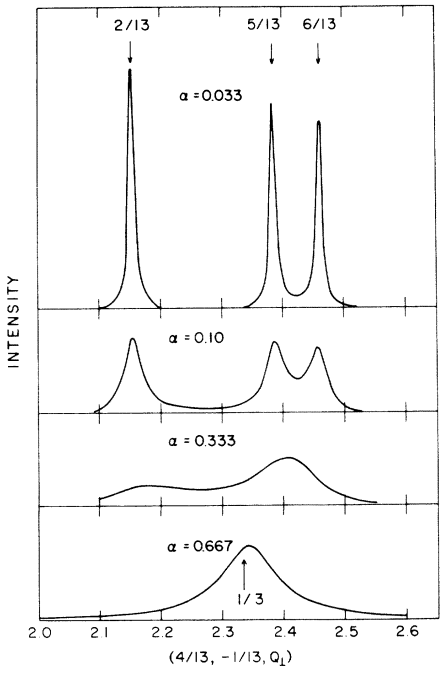

FIG. 5. Calculated scattering profiles show the deterioration of long-range order which occurs as the stacking fault probability α is increased.

We now discuss the details of these calculations. The CDW-induced displacements for the κth atom in the lth unit cell ($1T$ structure) in layer m are expressed as

$$\vec{u}_\kappa(l, m) = \sum_i \xi_{im} \vec{u}^i_\kappa(l) , \tag{1}$$

where the operator ξ_{im} is unity if layer m is in "configuration" i, and zero otherwise. The 13 possible "configurations" are given by $\vec{u}^i_\kappa(l)$, $i = 1, \ldots, 13$, which are obtained by translating the CDW displacement pattern centered on the origin (Ta-atom site 1, Fig. 3) by vectors $\vec{T}_i$. Thus the atomic displacements in configuration i are

$$\vec{u}^i_\kappa(l) = \sum_{\vec{q}} \vec{e}_\kappa(\vec{q}) e^{i\vec{q}\cdot(\vec{R}_l - \vec{T}_i)} + \text{c.c.} , \tag{2}$$

where the sum includes contributions from the three waves ($\vec{q}_1$, $\vec{q}_2$, and $\vec{q}_3$). Here $\vec{e}_\kappa(\vec{q})$ is the (complex) displacement eigenvector.

To leading order in displacement, the elastic scattering of the superlattice (i.e., $\vec{Q} \neq \vec{\tau}$) is given by

$$S(\vec{Q}) = \sum_{k, \vec{\tau}, \vec{q}} |f_{\vec{q}}(\vec{Q})|^2 \times \sum_{ij} [e^{\pm i\vec{q}\cdot(\vec{T}_i - \vec{T}_j)} G_{ij}(k)] \delta(\vec{Q} + \vec{\tau} \pm \vec{q} - k\hat{z}) , \tag{3}$$

where

$$|f_{\vec{q}}(\vec{Q})|^2 = \left| \sum_\kappa b_\kappa e^{i\vec{Q}\cdot\vec{r}_\kappa} \vec{Q}\cdot\vec{e}_\kappa(\vec{q}) \right|^2 . \tag{4}$$

In this expression, b_κ and $\vec{r}_\kappa$ are the coherent neutron-scattering length and the position respectively of the κth atom in the $1T$ unit cell. All information on the stacking order is contained in the disorder correlation function:

$$G_{ij}(k) \equiv \sum_{m, m'} e^{-i(m-m')k} \langle \xi_{im} \xi_{jm'} \rangle , \tag{5}$$

where $\langle\ \rangle$ denotes ensemble average. The function $\langle \xi_{im} \xi_{jm'} \rangle$ is the joint probability that layer m is in configuration i and layer m' is in configuration j. It may be expressed as

$$\langle \xi_{im} \xi_{jm'} \rangle = p P_{ij}(m' - m) , \tag{6}$$

where $p = \frac{1}{13}$, the probability of a given configuration occurring in any layer, and $P_{ij}(m' - m)$ is the conditional probability that layer m' is in configuration j when layer m is in configuration i. By translational invariance this probability depends only on the difference $M \equiv m' - m$, and we will write it as $P_{ij}(M)$ henceforth. Since Eq. (6) ensures that $P_{ji}(-M) = P_{ij}(M)$, we will take $M > 0$ in

the following analysis.

It is instructive to first assume that only nearest-layer interactions are important in determining the interlayer ordering. In this case we may write $P_{ij}(M)$ as the matrix product

$$P_{ij}(M) = \sum_{j_1, j_2, j_3, \cdots, j_{M-1}} P_{ij_1}(1) P_{j_1 j_2}(1) \times P_{j_2 j_3}(1) \cdots P_{j_{M-1} j}(1) = [\underline{P}(1)^M]_{ij}, \quad (7)$$

where $P_{ij}(1)$ is the probability of finding layer $m+1$ in configuration j if layer m is in configuration i. The elements of $P_{ij}(1)$ are determined by the nature and symmetry of the interlayer forces. We assume that only relative translations $\vec{T}_2$, $\vec{T}_4$, $\vec{T}_{10}$ are needed to explain the data in the impurity range of interest. Therefore, only three nonzero elements occur in any row of $P_{ij}(1)$. Since the translations associated with these elements are equivalent by trigonal symmetry, and conservation of probability requires

$$\sum_i P_{ij}(1) = 1,$$

every finite element in the matrix must be $\frac{1}{3}$. The full matrix is given by

$$P_{ij}(1) = \begin{cases} \frac{1}{3}, & \text{if } \vec{T}_{j-i+1} = \vec{T}_2, \vec{T}_4, \text{ or } \vec{T}_{10}, \\ 0, & \text{otherwise}. \end{cases} \quad (8)$$

Thus, if layer m is in configuration i, layer $m+1$ is equally likely to be a configuration given by translating the pattern in layer m by $\vec{T}_2$, $\vec{T}_4$, or $\vec{T}_{10}$, i.e., configurations $i+1$, $i+3$, or $i+9$ (modulo 13).

To calculate the disorder correlation function, we combine Eqs. (5), (6), and (7) to obtain the matrix equation

$$\underline{G}(k) = Np\left(\underline{I} + \sum_{M>0} [\underline{P}(k)^M + \underline{P}^\dagger(k)^M]\right), \quad (9)$$

where $\underline{I}$ is the unit matrix, N is the number of layers in the sample, and

$$\underline{P}(k) = e^{ik}\underline{P}(1). \quad (10)$$

Carrying out the summation in Eq. (9) we find

$$\underline{G}(k) = Np\{[\underline{I} - \underline{P}(k)]^{-1} + [\underline{I} - \underline{P}^\dagger(k)]^{-1} - \underline{I}\}. \quad (11)$$

We have used this form of $\underline{G}(k)$ in a computer calculation of $S(\vec{Q})$ [Eq. (3)]. To carry out this calculation we have had to assume reasonable values[12] for the displacement eigenvector components. However, the calculated profile is insensitive to this choice, except for normalization. Remarkably, the calculated profile [solid line in Fig. 2(b)] fits the data in the crystals with Zr concentrations $0.03 \leq x \leq 0.07$. The profile is broad, indicating the lack of long-range interlayer order. Since we have described a system with only nearest-layer interactions we draw two conclusions: (i) the development of long-range order must require longer-range interactions, between next-nearest layers for example; (ii) impurities can suppress these longer-range forces.

Physically it is clear that a system with only nearest-layer interactions will not have long-range order. Since there are three possible configurations for each layer which minimize its interaction energy with the preceding layer, the stacking is characterized by a random choice of translation vector $\vec{T}_2$, $\vec{T}_4$, or $\vec{T}_{10}$ in going from layer to layer. For systems with longer-range correlations (i.e., the $x = 0.015$ sample) we reformulate the problem to include the effects of next-nearest layer interactions. First we introduce the conditional probability $P_{ijk}(1,2)$ that layer $m+2$ is in configuration k given that layers m and $m+1$ are in configurations i and j respectively. Then the expression for $P_{ij}(M)$ analogous to Eq. (7) is

$$P_{ij}(M) = \sum_{j_1, j_2, j_3, \cdots, j_{M-1}} P_{ij_1}(1) P_{ij_1 j_2}(1,2) P_{j_1 j_2 j_3}(1,2) \cdots P_{j_{M-2} j_{M-1} j}(1,2). \quad (12)$$

The requirements of trigonal symmetry and conservation of probability, together with the stipulation that neighboring layers be related by one of the relative translation $\vec{T}_2$, $\vec{T}_4$, or $\vec{T}_{10}$, lead to the conclusion that all the elements of $P_{ijk}(1,2)$ may be expressed in terms of a single variable α, the "stacking-fault probability." The elements of $P_{ijk}(1,2)$ are assigned as follows:

(i) If the translation relating configurations j and k ($\vec{T}_{k-j+1}$) is *not* the same as that relating i and j ($\vec{T}_{j-i+1}$), but both vectors are from the set ($\vec{T}_2, \vec{T}_4, \vec{T}_{10}$), a stacking fault has occurred with probability $P_{ijk}(1,2) = \frac{1}{2}\alpha$.

(ii) If $\vec{T}_{k-j+1} = \vec{T}_{j-i+1} = \vec{T}_2$, $\vec{T}_4$, or $\vec{T}_{10}$, then a fault has not occurred and $P_{ijk}(1,2) = 1 - \alpha$.

(iii) Otherwise $P_{ijk}(1,2) = 0$.

To calculate the scattering profile $S(\vec{Q})$ as a function of α, we must evaluate the disorder-correlation function. The summation of Eq. (12) may be carried out to give

$$P_{ij}(M) = \sum_{j_1} P_{ij_1}(1) \sum_{\lambda} (\underline{R}^{M-1})_{\mu\nu} ,$$

where the matrix $\underline{R}$ is defined by

$$R_{\mu\nu} = P_{ij_1} \delta_{j_1\lambda} ,$$

with

$$\mu = 13(i-1) + j_1, \quad \nu = 13(\lambda - 1) + j .$$

Then the correlation function may be evaluated analytically, as we have done in Eqs. (9)–(11) for the case of nearest-layer interactions. Computer calculations of $S(\vec{Q})$ have been made for different values of α, as shown in Fig. 5. In the limit of small α, the scattering is that expected for domains of the three stacking translations $\vec{T}_2$, $\vec{T}_4$, $\vec{T}_{10}$, each having long-range order. At the other limit, $\alpha = \frac{2}{3}$, the profile is characteristic of a system with only nearest-layer interactions, since the probability of a given configuration is independent of the configuration of the next-nearest layer.[13]

IV. CONCLUSIONS

A consistent picture emerges to describe the effects of Zr impurities. The CDW superlattice can be characterized in terms of three domains, one for each relative stacking translation $\vec{T}_2$, $\vec{T}_4$, or $\vec{T}_{10}$. In the pure system these domains are of macroscopic size. As Zr is added, the number of stacking faults increases and the domain sizes are reduced. When $x = 0.015$, ordered sequences are, on average, at least 25 layers long. For concentrations $0.03 \leq x \leq 0.07$, the correlation length is independent of concentration at a value of about two layers.

We have shown that both nearest- and next-nearest-layer interactions are important in determining the interlayer order. The next-nearest-layer interaction is weak and rapidly overwhelmed by the addition of Zr impurities. The nearest layer interaction, which appears to be predominantly a Coulomb interaction between CDWs, is much stronger and continues to control the interlayer order in systems up to $x = 0.07$. Presumably much larger impurity concentrations would be necessary to override the nearest-layer coupling forces in order to further reduce the correlation length.

Although the interlayer correlations decrease rapidly with increasing impurity concentration, the CDW in the layer maintains reasonably long-range coherence. At higher impurity concentrations, the CDW structure should be driven in general from a commensurate to an incommensurate one, and finally with enough disorder the CDW instability might be suppressed completely.[5,6] In the present study, samples having an impurity concentration of $x = 0.05$ exhibit a coherent, commensurate CDW covering an area in the layer ($\xi_{\parallel}^2 = 1.2 \times 10^4$ Å^2) containing some 50 impurities. Thus, we can conclude that the locking energy, responsible for the commensurability of the superstructure in a single layer, is greater than the CDW-impurity interaction. In previous studies,[9] Zr impurity concentrations of $x = 0.08$ were needed to suppress the commensurate structure at 300 K. We hope to extend the present studies to measure the temperature dependence of both in-layer and interlayer impurity-induced disorder.

ACKNOWLEDGMENT

We thank P. Dernier for an x-ray-diffraction study of our samples.

---

*Work at Brookhaven performed under the auspices of the U. S. Energy Research and Development Administration.

†Supported in part by the NSF and the Alfred P. Sloan Foundation.

[1] J. W. Lynn, M. Iizumi, G. Shirane, S. A. Werner, and R. B. Saillant, Phys. Rev. B 12, 1154 (1975), and references therein.

[2] R. Comès, S. M. Shapiro, G. Shirane, A. F. Garito, and A. J. Heeger, Phys. Rev. Lett. 35, 1518 (1975), and references therein.

[3] J. A. Wilson, F. J. DiSalvo, and S. Mahajan, Adv. Phys. 24, 117 (1975); D. E. Moncton, J. D. Axe, and F. J. DiSalvo, Phys. Rev. Lett. 34, 734 (1975).

[4] L. J. Sham and B. R. Patton, Phys. Rev. Lett. 36, 733 (1976).

[5] W. L. McMillan, Phys. Rev. B 12, 1187 (1975).

[6] L. J. Sham and B. R. Patton, Phys. Rev. B (to be published).

[7] F. J. DiSalvo, R. G. Maines, and J. V. Waszczak, Solid State Commun. 14, 497 (1974).

[8] C. B. Scruby, P. M. Williams, and G. S. Parry, Philos. Mag. 31, 255 (1975).

[9] F. J. DiSalvo, J. A. Wilson, B. G. Bagley, and J. V. Waszczak, Phys. Rev. B 12, 2220 (1975).

[10] See charge contours of Fig. 31(a), Ref. 3.

[11] The powder x-ray-diffraction pattern of 1T-$TaSe_2$ in Refs. 3, 7 is fit with the unit cell: $\vec{a}' = 3\vec{a}_1 - \vec{a}_2$, $\vec{b}' = 4\vec{a}_2 + \vec{a}_1$, $\vec{c}' = \vec{c} + \vec{T}_2$. Lines have instrumental widths implying a correlation length longer than 500 Å.

[12] The Ta and Se atoms are displaced parallel to $\vec{a}_1^*$ with no motion along $\vec{c}^*$. These displacements are similar to those which occur in 2H-$TaSe_2$ below 120 K. (See Ref. 4.)

[13] For this value of α, the matrix $P_{ij}(M)$ calculated by Eq. (12) is identical to that calculated in Eq. (7) for the model having only nearest-layer interactions.